

6. TERRIGENOUS MATTER AND DISPERSED ASH IN SEDIMENT FROM THE CARIBBEAN SEA: RESULTS FROM LEG 165¹

Junenette L. Peters,² Richard W. Murray,² Joel W. Sparks,² and Drew S. Coleman²

ABSTRACT

Records of long-term sediment deposition in the Caribbean Sea were recovered during Ocean Drilling Program Leg 165. Samples from the Cayman Rise (Site 998), the Colombian Basin (Site 999), and the Hess Escarpment (Site 1001) were analyzed for calcium carbonate (CaCO₃) by coulometry and for selected major and trace elements by X-ray fluorescence and inductively coupled plasma-emission spectrometry. These data were used to quantify in the bulk sediment the absolute concentrations of CaCO₃, terrigenous matter, and dispersed ash (as opposed to discrete ash layers). The weight percent of terrigenous matter was computed using a Cr-based normative calculation, and dispersed ash content was calculated by difference; the assumption of a three component system (CaCO₃, ash, and terrigenous matter) is justified by and consistent with petrographic analysis.

Sites 998 and 999 broadly exhibit the same pattern of terrigenous accumulation. Both show a general decrease in terrigenous accumulation rates during the Oligocene and early Miocene, except for a sharp increase at Site 998 during the early Oligocene (30–40 Ma) and significant increases in the late Miocene and late Pliocene/early Pleistocene. The same pattern in terrigenous accumulation is recorded at Sites 925 and 929 in the Ceara Rise (Atlantic Ocean), which receives input from an Amazon River source, demonstrating that Sites 925, 929, 998, and 999 collectively provide a circum-Andean record of tectonic uplift, with the Leg 165 sites responding to inputs from the Magdalena River system. Both Sites 998 and 999 appear to be responding to South and Central American inputs, particularly after the middle Miocene; however, the variation in the terrigenous, carbonate, and dispersed ash at Site 998 point to an erosional event during the Oligocene that is apparently unique to this site's location.

Dispersed ash commonly accounts for 15–20 wt% of the bulk sediment, and in some cases up to 45 wt%. The accumulation of dispersed ash typically leads the accumulation of discrete layers by 2–10 m.y. These changes in sediment composition could signify (1) the distance from the source of volcanism, (2) periods of small volume volcanic activity preceding the large eruptions, or (3) the transportation to the deep sea of terrestrially deposited ash preceding the large eruptions.

INTRODUCTION

The accumulation and composition of sediment preserved on the deep-ocean floor reflects the tectonic evolution, volcanic history, climate changes, and weathering rates of the nearby continental regions. The terrigenous and volcanic components of the sediment result from physical and chemical weathering that act on the exposed crustal rocks at any particular time period in Earth's history. Studying the chemical composition of terrigenous matter in deep-sea sediment can help to answer questions of how sediment is weathered and transported, address the composition and geographic location of the sediment source(s), and contribute to our understanding of regional and global chemical mass balances.

The Caribbean region is an opportune place to study these and other topics for several reasons. First, the Caribbean Sea region is unlike other Atlantic-type ocean basins. The Caribbean plate is allochthonous with respect to its neighbors, making it difficult to reconstruct its paleogeology. For example, there are many models of the plate tectonic evolution of the Gulf of Mexico and the Caribbean, all of which are inconclusive in some regard (Burke et al., 1978; Duncan and Hargraves, 1984; Burke, 1988; Donnelly, 1989; Pindell and Barrett, 1990; Morris et al., 1990). In this context, the past volcanic activity in the region is not thoroughly known. Secondly, the region

(Fig. 1) holds a central tectonic and geographic position because it lies between the North and South American plates and the Pacific and Atlantic Oceans. Accordingly, it played a vital role in global ocean circulation until the closing of the Isthmus of Panama, which began at ~13 Ma and was completed at ~1.9 Ma (Farrell et al., 1995, and references therein). Return flow from the South Atlantic that feeds the Gulf Stream moves through the Caribbean, and paleoceanographic studies of carbonate preservation (e.g., Droxler and Burke, 1995) illustrate the Caribbean's important geographic location today.

For ~20 yr before Leg 165, there was no recovery of deeply buried sediment in the circum-Caribbean region. Five sites were drilled during Leg 165, and, of these, we discuss chemical records from Sites 998, 999, and 1001 here. These sites cover nearly 80 m.y. of Earth's history (Sigurdsson, Leckie, Acton, et al., 1997). The two sites visited during Leg 165 and not discussed here (Sites 1000 and 1002) have unique characteristics that make them inapplicable to this study: Site 1000 is a drowned carbonate platform (Droxler et al., 1998) and Site 1002 is a large anoxic marine basin (Cariaco Basin) with only a 600,000 yr record (Peterson et al., 1998).

Our results indicate that throughout the region the sediment is dominated by the calcium carbonate (CaCO₃) fraction. The noncarbonate fraction is composed of detrital sediment (hereafter referred to as "terrigenous") and dispersed ash. Dispersed ash is different from discrete ash layers (Carey and Sigurdsson, 1998; Carey and Sigurdsson, Chap. 5, this volume) and refers to ash that is physically and chemically mixed with the carbonate and other noncarbonate sediments. In this paper, we use the bulk sediment chemistry to quantitatively determine the absolute percentages of CaCO₃, terrigenous matter, and dispersed ash in the sediment sequences at the three sites. We

¹Leckie, R.M., Sigurdsson, H., Acton, G.D., and Draper, G. (Eds.), 2000. *Proc. ODP, Sci. Results*, 165: College Station, TX (Ocean Drilling Program).

²Department of Earth Sciences, Boston University, Boston, MA 02215, U.S.A. Murray: rickm@bu.edu

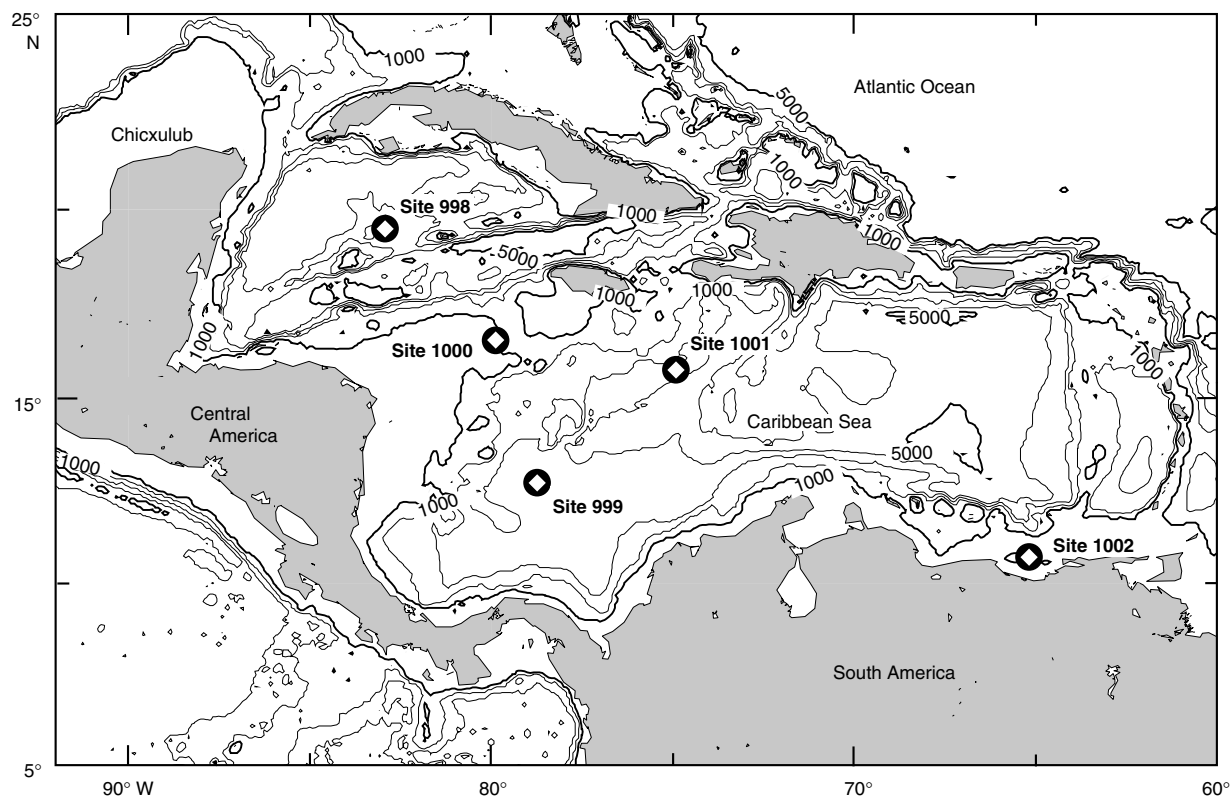


Figure 1. Location map of sites drilled during Leg 165. Of the sites discussed here, Site 998 is located on the Cayman Rise ($19^{\circ}29.377'N$, $82^{\circ}56.166'W$, 3179.9 m water depth) and is flanked to the north by Yucatan Basin and to the south by the Cayman Ridge and Cayman Trough. Site 999 is located in the Colombian Basin, on what is now named the Kogi Rise ($12^{\circ}44.639'N$, $78^{\circ}44.360'W$, 2827.9 m water depth), ~150 km northeast of the Mona Rise. Site 1001 is in the lower Nicaraguan Rise on the Hess Escarpment ($15^{\circ}45.427'N$, $74^{\circ}54.627'W$, 3259.6 m water depth) (from Sigurdsson, Leckie, Acton, et al., 1997). Sites 925 and 929 are located off the map to the east in the Amazon River Basin.

will discuss the temporal and paleogeographic changes in terrigenous supply, the timing and magnitude of increases and decreases in the accumulation of dispersed ash, and interpret the paleoceanographic patterns in the context of the changing tectonics of the Cenozoic Caribbean Sea.

METHODS

Coring and Stratigraphy

Details of the coring procedures, the use of planktonic foraminifers and calcareous nannofossil datums and magnetostratigraphic polarity zone boundaries to obtain sedimentation rates, and calculations of the bulk accumulation rates may be found in Sigurdsson, Leckie, Acton, et al. (1997).

The age-to-depth and mass accumulation rates for each sample were calculated using interpolated ages for each core interval. Although our records cover approximately the last 80 m.y., in some cases they are not complete. At Site 1001, middle Miocene nannofossil ooze overlies middle Eocene chalk, and the middle Eocene chalk overlies early Eocene chalk, corresponding to hiatuses of 30 and 8 m.y., respectively (Sigurdsson, Leckie, Acton, et al., 1997).

Normative Calculations of Sediment Composition

The absolute concentration of the terrigenous component was obtained from normative calculations based on the concentration of Cr in a given sample and the concentration of Cr in average shale (Table 1; Cr \approx 110 ppm; Taylor and McLennan, 1985) according to

$$(\% \text{Terrigenous})_{\text{sample}} = 100 \times (Cr_{\text{sample}}) / (Cr_{\text{average shale}}).$$

This calculation compares the composition of a given sample to that of an "average shale." In Sigurdsson, Leckie, Acton, et al. (1997), the terrigenous component at Site 998 was calculated using a model-based Ti/Zr value. Although there are no significant differences in results from these two methods, the terrigenous component was recalculated here using the Cr-based normative approach for consistency. We use the value of Cr for average shale based on the Post Archean Average Shale (PAAS) of Taylor and McLennan (1985). Although this is a somewhat arbitrary choice, it is important to note that other average shales (e.g., North American Shale Composite with Cr \approx 125 ppm, Gromet et al., 1984; Proterozoic and Phanerozoic cratonic shales with Cr \approx 110 ppm, Condie, 1993; Continental Crust with Cr = 119 ppm, Rudnick and Fountain, 1995) have similar concentrations of Cr. In further support of our selection of this particular Cr concentration, we note that Dobson et al. (1997) determined the chemical composition of operationally derived (i.e., using a sequential extraction procedure) terrigenous matter at the Ceara Rise, thought to represent sediment transported down the Amazon River, and the average of their determinations yields Cr \approx 100 ppm. Thus, the results described below are not overly dependent on the choice of any particular average shale approximation.

Chromium was selected as the reference element because a large majority of the discrete ash layers contain <3 ppm Cr (Sigurdsson, Leckie, Acton, et al., 1997), compared to 110 ppm in average shale (Taylor and McLennan, 1985). Thus, given these end-member values, even in a sediment sample with a large amount of dispersed ash and a small terrigenous load, the use of Cr to quantitatively determine

Table 1. Composition of Leg 165 sediments, based on shipboard XRF and coulometry.

Core, section, interval (cm)	Depth (mbsf)	Age (Ma)	Cr (ppm)	Carbonate (wt%)	Terrigenous (wt%)	Ash (wt%)	Accumulation rate		
							Carbonate (g/cm ² /k.y.)	Terrigenous (g/cm ² /k.y.)	Ash (g/cm ² /k.y.)
165-998A-									
1H-2, 28-30	1.78	ND	22	74	20	6	ND	ND	ND
1H-6, 33-35	7.83	ND	20	73	18	9	ND	ND	ND
2H-3, 27-29	12.07	0.65	14	84	13	3	1.61	0.24	0.06
2H-5, 27-29	15.07	0.81	17	76	15	9	1.36	0.28	0.15
3H-5, 33-35	24.63	1.31	21	75	19	6	1.34	0.34	0.11
4H-2, 27-29	29.57	1.58	34	66	31	3	1.21	0.57	0.06
4H-5, 27-29	34.07	1.82	26	69	24	7	1.32	0.45	0.14
5H-1, 27-29	37.57	2.00	16	79	15	6	1.61	0.30	0.13
6H-1, 28-30	47.08	2.51	21	79	19	2	1.58	0.38	0.04
7H-2, 50-51	58.30	3.10	18	78	16	6	1.64	0.34	0.12
8H-2, 110-112	68.40	3.63	24	75	22	3	1.58	0.46	0.07
9H-2, 37-39	77.17	4.09	18	78	16	6	1.76	0.37	0.13
10H-5, 100-102	91.80	4.87	19	78	17	5	1.69	0.38	0.10
11H-4, 28-30	99.08	5.26	25	73	23	4	1.60	0.50	0.09
12H-4, 26-28	108.56	6.04	28	71	25	4	0.76	0.27	0.04
13H-1, 27-29	113.57	6.66	41	56	37	7	0.60	0.40	0.07
13H-4, 27-29	118.12	7.22	36	55	33	12	0.59	0.35	0.13
14H-1, 26-28	123.06	7.84	15	74	14	12	0.71	0.13	0.12
15H-1, 27-29	132.57	9.00	12	83	11	6	0.89	0.12	0.07
16H-1, 27-29	142.07	10.18	13	74	12	14	0.69	0.11	0.13
16H-4, 28-30	146.58	10.74	81	12	74	14	0.11	0.67	0.13
17H-1, 26-28	151.56	11.35	83	BDL	75	25	BDL	0.59	0.19
18X-4, 10-12	165.40	13.06	12	74	11	15	0.67	0.10	0.14
19X-4, 28-30	170.98	13.77	13	77	12	11	1.44	0.22	0.21
20X-1, 29-31	176.19	14.10	9	77	8	15	1.15	0.12	0.22
21X-1, 40-42	185.90	14.71	9	74	8	18	1.36	0.15	0.33
21X-4, 42-44	190.42	14.98	4	88	4	8	1.67	0.07	0.16
23X-4, 31-33	209.61	16.18	5	ND	5	ND	ND	0.08	ND
25X-4, 10-12	228.60	17.37	4	86	4	10	1.44	0.06	0.17
27X-4, 41-43	248.11	18.59	5	ND	5	ND	ND	0.10	ND
29X-1, 27-29	262.77	19.51	7	82	6	12	1.75	0.14	0.25
33X-1, 54-56	301.44	21.92	3	91	3	6	1.85	0.06	0.13
38X-2, 62-64	351.12	24.65	3	92	3	5	3.17	0.09	0.18
41X-2, 99-100	380.39	25.87	4	ND	4	ND	ND	0.13	ND
48X-2, 49-51	447.29	28.64	ND	93	ND	ND	3.03	ND	ND
53X-1, 27-29	493.57	30.56	3	91	3	6	3.22	0.10	0.22
60X-3, 62-64	564.32	33.50	4	88	4	8	3.24	0.13	0.31
61X-1, 45-47	570.75	33.76	4	88	4	8	3.18	0.13	0.30
62X-1, 65-67	580.55	34.17	8	87	7	6	3.52	0.29	0.23
63X-1, 0-2	589.50	34.54	10	ND	9	ND	ND	0.37	ND
65X-1, 28-30	608.98	35.35	6	ND	5	ND	ND	0.23	ND
165-998B-									
11R-1, 47-49	654.97	37.34	4	89	4	7	2.54	0.10	0.21
165-999A-									
1H-3, 77-79	3.77	0.11	80	31	73	BDL	0.78	1.82	BDL
2H-3, 127-129	11.87	0.36	56	46	51	3	1.27	1.40	0.09
3H-5, 7-9	23.17	0.69	61	48	55	BDL	1.39	1.60	BDL
4H-3, 53-55	30.13	0.90	77	34	70	BDL	1.12	2.31	BDL
5H-3, 112-114	40.22	1.20	75	35	68	BDL	1.11	2.17	BDL
6H-4, 3-5	50.13	1.49	58	42	53	5	1.25	1.57	0.16
7H-5, 30-32	61.40	1.83	55	48	50	2	1.57	1.64	0.07
8H-3, 97-99	68.57	2.04	51	49	46	5	1.56	1.48	0.15
9H-3, 77-79	77.87	2.32	37	57	34	9	1.78	1.05	0.29
10H-2, 82-84	85.92	2.56	38	60	35	5	1.72	0.99	0.16
11H-3, 7-9	96.17	2.87	36	56	33	11	1.54	0.90	0.31
12H-3, 49-51	106.09	3.20	38	50	35	15	1.12	0.78	0.35
13H-1, 88-90	112.98	3.43	36	57	33	10	1.64	0.94	0.30
14H-4, 128-130	127.38	3.91	37	59	34	7	1.75	1.00	0.22
15H-2, 77-79	133.37	4.11	43	51	39	10	1.49	1.14	0.29
16H-3, 97-99	144.57	4.48	47	46	43	11	1.54	1.43	0.38
17H-3, 92-94	154.02	4.61	45	50	41	9	0.87	0.72	0.16
18H-2, 97-99	162.07	5.03	26	67	24	9	1.46	0.52	0.20
19H-2, 78-80	171.38	5.51	33	57	30	13	1.17	0.61	0.27
21H-5, 92-94	195.02	6.75	44	48	40	12	1.06	0.88	0.27
22X-2, 78-80	199.88	7.00	32	54	29	17	1.14	0.62	0.36
23X-1, 144-146	202.04	7.12	31	63	28	9	1.34	0.60	0.19
24X-4, 98-100	215.78	7.84	37	50	34	16	1.10	0.74	0.36
25X-4, 101-103	225.41	8.35	40	48	36	16	0.72	0.55	0.24
26X-1, 98-100	230.48	8.61	33	53	30	17	0.91	0.52	0.29
27X-4, 127-129	244.87	9.36	37	53	34	13	1.14	0.72	0.29
29X-1, 127-129	259.67	10.14	35	55	32	13	1.15	0.66	0.27
29X-6, 13-15	266.03	10.47	89	11	81	8	0.25	1.85	0.19
30X-2, 128-130	270.78	10.72	54	37	49	14	0.81	1.07	0.30
30X-7, 18-20	277.18	11.06	97	10	88	2	0.22	1.96	0.04
31X-5, 126-128	284.86	11.46	116	2	105	BDL	0.04	2.28	BDL
32X-5, 89-91	294.09	11.94	61	32	55	13	0.73	1.26	0.29
33X-5, 87-89	303.57	12.44	34	51	31	18	0.94	0.57	0.33
34X-3, 90-92	310.20	12.78	40	40	36	24	0.68	0.62	0.40
36X-2, 97-99	328.07	13.72	30	50	27	23	1.03	0.56	0.47
37X-6, 102-104	343.72	14.54	18	53	16	31	1.14	0.35	0.66
39X-1, 129-131	355.69	15.17	12	71	11	18	1.65	0.25	0.42
40X-3, 97-99	367.97	15.74	20	63	18	19	2.39	0.69	0.71
42X-4, 129-131	389.19	16.45	13	71	12	17	2.65	0.44	0.64
43X-3, 77-79	396.77	16.71	13	66	12	22	2.36	0.42	0.79

Table 1 (continued).

Core, section, interval (cm)	Depth (mbsf)	Age (Ma)	Cr (ppm)	Carbonate (wt%)	Terrigenous (wt%)	Ash (wt%)	Accumulation rate		
							Carbonate (g/cm ² /k.y.)	Terrigenous (g/cm ² /k.y.)	Ash (g/cm ² /k.y.)
45X-4, 99-100	417.59	17.41	15	62	14	24	2.28	0.50	0.89
47X-5, 79-81	438.19	18.12	7	75	6	19	3.13	0.27	0.78
47X-5, 81-83	438.21	18.12	7	74	6	20	3.09	0.27	0.82
48X-5, 119-121	448.29	18.45	10	71	9	20	2.88	0.37	0.81
50X-3, 84-86	464.14	19.00	12	55	11	34	2.39	0.47	1.48
51X-4, 127-129	475.67	19.38	9	70	8	22	2.82	0.33	0.88
52X-1, 101-103	480.51	19.54	11	57	10	33	2.28	0.40	1.32
53X-5, 82-84	495.92	20.07	10	67	9	24	3.06	0.41	1.09
54X-3, 104-106	502.74	20.30	8	69	7	24	3.25	0.34	1.12
55X-CC, 7-9	508.37	20.50	14	62	13	25	3.24	0.67	1.32
56X-CC, 6-8	513.88	20.68	12	68	11	21	3.77	0.60	1.17
57X-CC, 10-12	518.31	20.83	14	70	13	17	3.25	0.59	0.80
58X-5, 30-32	533.90	21.36	10	57	9	34	2.53	0.40	1.51
59X-1, 37-39	537.57	21.48	9	66	8	26	3.06	0.38	1.20
60X-4, 58-60	551.88	21.96	8	66	7	27	3.24	0.36	1.31
61X-3, 92-94	560.42	22.26	6	75	5	20	3.69	0.27	0.96
165-999B-									
5R-2, 24-26	574.30	22.73	5	71	5	24	4.67	0.30	1.61
6R-1, 75-77	577.95	22.85	12	65	11	24	4.13	0.69	1.53
8R-2, 28-30	593.58	23.38	10	69	9	22	4.56	0.60	1.45
9R-5, 93-95	607.10	23.93	8	62	7	31	1.63	0.19	0.81
10R-1, 31-33	611.41	24.27	8	72	7	21	2.05	0.21	0.59
11R-3, 98-100	624.15	25.27	9	70	8	22	1.98	0.23	0.62
12R-5, 75-77	635.70	26.18	7	72	6	22	2.09	0.18	0.63
13R-4, 9-11	644.49	26.87	4	81	4	15	2.38	0.11	0.45
15R-2, 72-74	661.32	28.20	6	72	5	23	2.10	0.16	0.66
19R-1, 58-61	682.48	29.86	BDL	84	BDL	16	2.51	0.00	0.48
20R-1, 57-59	685.47	30.10	4	87	4	9	2.54	0.11	0.27
21R-3, 117-119	692.07	30.62	BDL	79	BDL	21	2.38	0.00	0.63
22R-3, 81-83	701.41	31.35	4	80	4	16	2.42	0.11	0.50
23R-1, 102-104	708.22	31.89	4	70	4	26	2.17	0.11	0.82
24R-3, 69-71	720.39	32.85	3	72	3	25	2.04	0.08	0.72
26R-5, 84-86	743.14	34.64	ND	ND	ND	ND	ND	ND	ND
27R-3, 41-43	749.39	35.14	4	72	4	24	2.23	0.11	0.75
28R-4, 79-81	760.99	36.05	BDL	73	BDL	27	2.08	0.00	0.77
29R-5, 93-95	772.33	36.97	BDL	78	BDL	22	1.75	0.00	0.49
31R-2, 2-4	786.42	40.57	BDL	76	BDL	24	2.53	0.00	0.80
32R-2, 46-48	796.26	41.26	BDL	62	BDL	38	2.16	0.00	1.32
33R-5, 30-32	811.00	42.29	BDL	87	BDL	13	3.08	0.00	0.46
34R-3, 35-38	817.85	42.77	5	61	5	34	2.21	0.16	1.25
36R-2, 63-65	835.83	44.02	BDL	83	BDL	17	2.93	0.00	0.60
38R-3, 105-107	856.95	45.50	BDL	67	BDL	33	2.23	0.00	1.10
39R-3, 83-85	866.43	46.17	BDL	73	BDL	27	2.62	0.00	0.97
40R-4, 53-56	877.23	46.92	BDL	82	BDL	18	2.91	0.00	0.64
41R-2, 69-71	884.09	47.40	5	77	5	18	2.81	0.17	0.67
42R-2, 79-81	888.79	47.72	10	51	9	40	1.41	0.25	1.10
44R-3, 112-114	905.22	48.88	12	54	11	35	1.86	0.38	1.21
45R-5, 63-66	917.33	49.72	15	54	14	32	1.76	0.45	1.06
46R-1, 120-122	921.50	50.02	13	47	12	41	1.46	0.37	1.28
47R-2, 122-124	932.72	50.80	40	47	36	17	1.41	1.09	0.50
48R-5, 81-83	946.41	51.76	17	57	15	28	1.93	0.52	0.93
49R-3, 67-68	952.87	52.28	25	65	23	12	1.47	0.51	0.28
50R-4, 97-99	964.27	53.52	21	70	19	11	1.41	0.39	0.22
51R-2, 142-144	971.32	54.29	17	67	15	18	1.55	0.36	0.41
52R-3, 4-6	981.14	55.35	29	62	26	12	1.40	0.60	0.26
53R-4, 96-98	991.83	56.52	20	59	18	23	1.34	0.41	0.52
54R-3, 116-118	1001.56	57.58	18	63	16	21	1.36	0.35	0.45
55R-5, 23-25	1013.33	58.86	34	60	31	9	1.22	0.63	0.18
56R-4, 65-67	1021.85	59.78	18	73	16	11	1.69	0.38	0.25
57R-3, 65-67	1029.95	61.57	4	77	4	19	1.01	0.05	0.25
58R-5, 75-77	1042.15	63.62	6	55	5	40	0.81	0.08	0.58
61R-5, 59-61	1061.69	65.70	4	89	4	7	2.12	0.09	0.18
62R-CC, 17-19	1066.45	66.21	4	87	4	9	2.09	0.09	0.22
165-1001A-									
2R-1, 42-44	6.82	ND	44	ND	40	ND	ND	ND	ND
3R-1, 110-112	17.20	1.20	41	58	37	4	0.82	0.52	0.06
6R-1, 145-150	46.35	3.22	55	57	50	BDL	0.80	0.70	BDL
9R-1, 145-150	75.25	5.23	45	54	41	5	0.76	0.58	0.07
11R-4, 98-100	98.48	6.84	51	60	46	BDL	0.98	0.76	BDL
12R-3, 145-150	107.05	7.44	56	57	51	BDL	1.00	0.90	BDL
15R-3, 145-150	135.95	9.44	51	55	46	BDL	0.90	0.76	BDL
17R-4, 98-100	156.18	12.17	19	72	17	11	0.54	0.13	0.08
18R-1, 145-150	161.75	13.00	14	65	13	22	0.49	0.10	0.17
18R-4, 98-100	165.78	19.36	4	68	4	28	0.75	0.04	0.32
21R-1, 84-86	180.44	52.56	8	62	7	31	1.64	0.19	0.82
24R-1, 86-88	209.26	54.08	4	66	4	30	2.01	0.11	0.93
28R-1, 58-60	247.48	56.11	6	73	5	22	2.09	0.16	0.63
34R-3, 145-150	309.05	59.36	8	74	7	19	2.04	0.20	0.52
36R-1, 145-150	325.25	60.22	12	71	11	19	2.47	0.38	0.65
36R-4, 43-45	328.73	60.41	8	60	7	32	2.14	0.26	1.15
40R-3, 0-5	365.30	65.87	9	76	8	16	1.41	0.15	0.29
43R-4, 109-111	396.79	69.15	3	90	3	8	1.98	0.06	0.17
46R-2, 47-49	421.97	71.48	3	93	3	5	2.20	0.06	0.11
51R-3, 93-95	471.61	76.08	3	95	3	2	2.22	0.06	0.06

Notes: ND = not determined, BDL = below detection limit. See text for description of analyses.

the terrigenous abundance is appropriate. Furthermore, as a refractory element, Cr is unlikely to be affected by diagenetic remobilization (Taylor and McLennan, 1985). Our use of Cr assumes that the original chemistry of the dispersed ash was similar to that of the discrete ash layers, at least with respect to Cr. The use of major elements such as Al or Ti to calculate the terrigenous load leads to erroneous results because these elements are found in large concentrations in both average shale (Taylor and McLennan, 1985) and Caribbean ash (Sigurdsson, Leckie, Acton, et al., 1997). Similarly, the use of other trace elements found in relatively low abundance in ash is precluded. For example, Ni was not chosen because the range of Ni concentrations in the ash layers is 30–90 ppm even in relatively unaltered ash (those with low MgO concentrations; Sigurdsson, Leckie, Acton, et al., 1997) and the concentration in average shale is 54 ppm (Taylor and McLennan, 1985). Vanadium was not chosen for the same reason; the V concentration in the ash (1–50 ppm) is not significantly lower than that of average shale (100 ppm).

Dispersed ash was calculated by difference according to

$$(\% \text{Ash})_{\text{sample}} = 100 - \% \text{CaCO}_3 - \% \text{Terrigenous}.$$

This yields a maximum estimate for the dispersed ash because the calculation could potentially include oxide and biogenic opal components in the remaining portion, as well as sea salt. However, Fe and Mn oxides and biogenic opal components only account for a maximum of 7% of the bulk sediment deposited here (Sigurdsson, Leckie, Acton, et al., 1997). Because such additional components may have stratigraphically local importance, care is taken to not overly rely on single data points.

Our normative calculations are in close agreement with petrographic analysis of the sediment. For example, at certain stratigraphic horizons where petrographic analysis indicates only the presence of terrigenous matter and CaCO_3 , our normative calculations yield numerical closure. Our calculations also agree with the qualitative smear-slide descriptions of the lithology (Sigurdsson, Leckie, Acton, et al., 1997). We estimate the uncertainty in the normative calculation of dispersed ash to be ~5%–10% of the measured weight percent value. We arrive at this estimate because of the ~3 ppm Cr in ash compared to the 110 ppm Cr in PAAS (3/110 ≈ 3%), as well as analytical precision of the Cr analysis (<2% of the measured value), the potential for variation in the detrital component, and when taking into consideration that other components are not necessarily included in the “by difference” calculation. Given the arithmetic, the realistic “detection

limit” of the normative approach is also ~5 wt% dispersed ash. All data are given in Table 1.

Chemical Analyses

Shipboard analysis of selected major and trace elements was performed by X-ray fluorescence (XRF). For Site 998, analysis was done on two samples per core for the first 150 meters below seafloor (mbsf) and then one per core below. At Site 999, samples were analyzed at a frequency of one per core, and at Site 1001, one sample every three cores. Samples were selected from intervals that appeared representative (so called “background” sediment) and had no obvious marker beds. Details of the shipboard analytical procedures may be found in Sigurdsson, Leckie, Acton, et al. (1997). Eighty-seven samples (~30 per site) were selected for reanalysis by inductively coupled plasma source emission spectrometry (ICP-ES) at Boston University to compare the shipboard XRF-generated data with ICP-ES. The ICP-ES analytical procedures were similar to those used by Schroeder et al. (1997), Murray and Leinen (1993, 1996), and Murray et al. (1995). Samples targeted for replicate analysis were chosen to bracket a range of Cr, Ti, and CaCO_3 concentrations. The shore-based ICP-ES analyses confirmed the shipboard XRF data determinations. Although shipboard XRF quality control was maintained at the highest possible level, including blind replicate analyses, the replicate analyses by the different technique gives us increased confidence in the analytical results.

RESULTS AND DISCUSSION

Overview

At all three sites, there is a high concentration of CaCO_3 with lower concentrations of terrigenous matter and dispersed ash (Fig. 2). The concentration of CaCO_3 varies between 0 and 80 wt% of the bulk sediment, with an average ~70 wt%. The extremely low concentrations of carbonate at Sites 998 and 999 at ~12 Ma define the “carbonate crash” discussed elsewhere (Farrell et al., 1995; Lyle et al., 1995; Roth et al., Chap. 17, this volume). Terrigenous matter concentrations average ~20 wt%, yet increase in the last 10 m.y. to ~35 wt%. This increase does not appear to be solely caused by the decrease in the amount of dispersed ash (i.e., is not caused solely by dilution), because the terrigenous accumulation rates also show a marked increase in this time interval (as discussed below). Overall there is a significant amount of dispersed ash, reaching a maximum value of 45 wt% of the

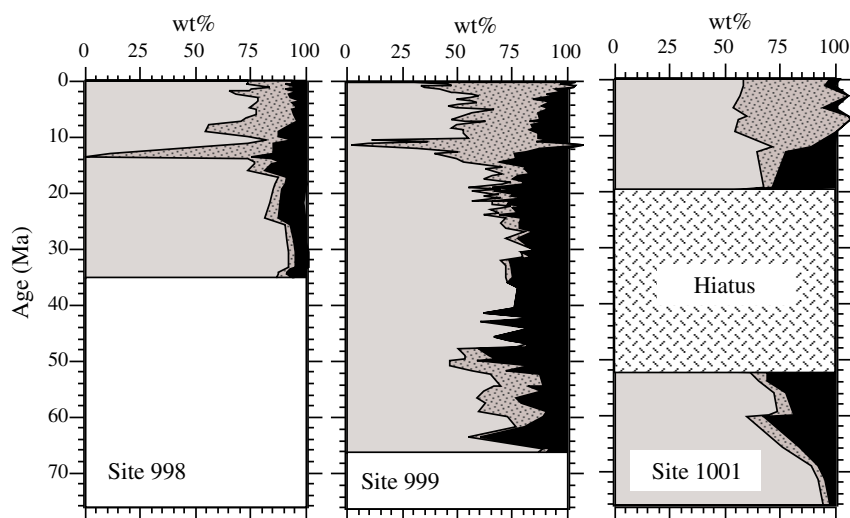


Figure 2. Absolute concentrations (in weight percent) of CaCO_3 (light gray), terrigenous matter (dark gray with spots), and dispersed ash (black) at Sites 998, 999, and 1001 plotted vs. age (Ma). Note hiatus at Site 1001.

bulk sediment. This is especially true before 10 Ma, where dispersed ash averages 18 wt%; after 10 Ma, dispersed ash only averages 5 wt% (i.e., near the detection limit of the normative calculation).

Site 999 generally shows the greatest mass accumulation rates of all three sediment components with two exceptions (Fig. 3). During the mid-Oligocene (between 36 and 24 Ma), CaCO_3 and terrigenous accumulation rates are greater at Site 998 than at Site 999 and reach to more than three times greater in the terrigenous component and 1.5 times greater in the CaCO_3 component. Also, between 60 and 62 Ma, Site 1001 has greater CaCO_3 and dispersed ash accumulation rates than Site 999 by ~1.5 and two times, respectively. Details of the variations in these components, as well as their interrelationships and tectonic significance, are discussed below.

Terrigenous Component

Sites 999 and 1001 record maxima in terrigenous matter accumulation rates at ~59 Ma (Fig. 4). At Site 999 these relatively high accumulation rates are maintained until ~50 Ma, whereas at Site 1001 the terrigenous accumulation reaches a maximum. Notwithstanding the caution needed in interpreting single data points, it appears that even at Site 1001 several points define an increase up to the maximum at

59 Ma and the decrease down from it. Site 999 shows low accumulation rates between 48 and 28 Ma, with essentially zero terrigenous accumulation between 46 and 32 Ma. Much of this time period of ultra-low terrigenous accumulation at Site 999 corresponds with the hiatus at Site 1001, which may reflect a regional depositional pattern. Between 28 and 6 Ma, Site 999 shows a steady increase in terrigenous accumulation (with the exception of the “carbonate crash”). Site 998 also shows a period of low accumulation rates in the Oligocene through the middle Miocene except for an increase in terrigenous accumulation at ~34 Ma. This event may reflect uplift in Guatemala (Weyl, 1980) that began during the Oligocene and increased through middle Miocene orogeny (Morris et al., 1990). Such uplift may be associated with the left-lateral offset between North America and the Caribbean as evidenced by the Oligocene-aged initial opening of Cayman Trough (Mann et al., 1990). At Sites 998 and 999, there is a significant maximum in terrigenous accumulation at ~12 Ma, which is not seen at Site 1001, and is related to the carbonate crash.

Most significantly, all three sites show a broad pattern of increased terrigenous matter (Fig. 2) and in terrigenous accumulation (Fig. 4) in sediment younger than 10 Ma. Sites 998 and 999 also record a maximum in terrigenous accumulation in the Pliocene at ~5 Ma and again at 1 Ma. In general, Sites 998 and 999 seem to be re-

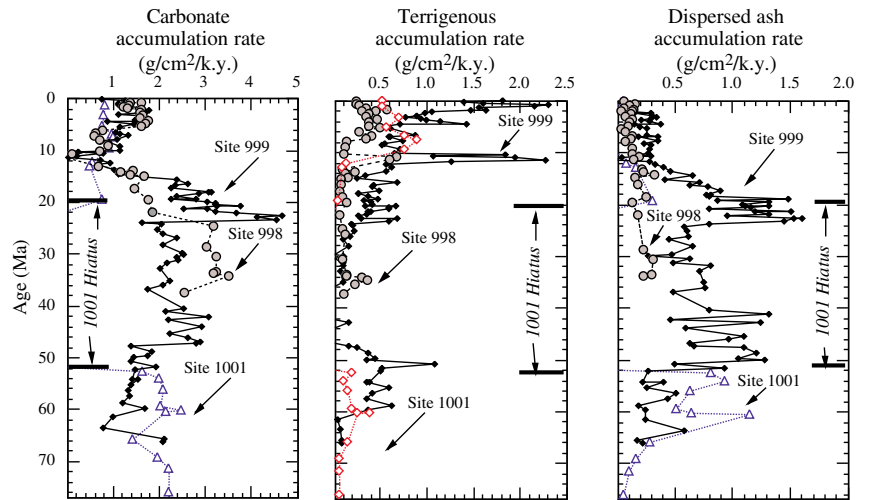


Figure 3. Carbonate, terrigenous, and dispersed ash accumulation rates at Site 998 (gray circles), Site 999 (black diamonds), and Site 1001 (open triangles) vs. age. Position of the hiatus at Site 1001 is marked on the age axis.

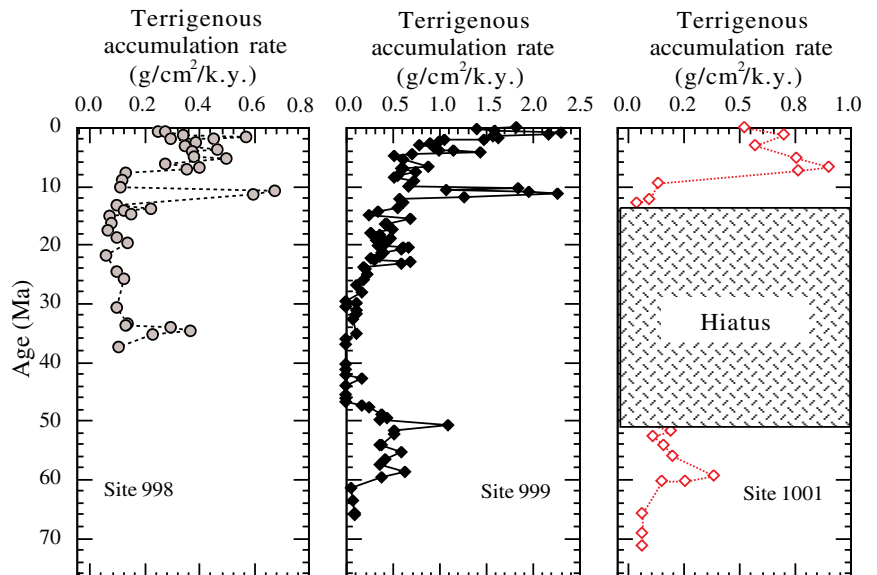


Figure 4. Terrigenous matter accumulation at Sites 998, 999, and 1001 vs. age, plotted with expanded scales on the x-axes.

sponding to the same input(s), especially since the late Miocene. The high terrigenous matter accumulation rates over the last 10 m.y. correspond with several orogenic events. From the late Miocene to the present, the final postorogenic phase in Guatemala, southern Central America, and northwestern South America has been characterized by uplift, deposition, and the advent of volcanism (Escalante, 1990; Morris et al., 1990; Mann et al., 1990; Mann and Burke, 1984).

Increases in terrigenous input over the past 10 m.y. are also recognized at Sites 925 and 929 located on the Ceara Rise (Dobson et al., 1997). Only carbonate and terrigenous matter (i.e., not ash) were studied at these Ceara Rise sites. Dobson et al. (1997) determined mass accumulation rates for the terrigenous component by using the calculated weight percent values determined from an operationally derived sequential extraction, shipboard discrete density measurements, and a biostratigraphic time scale. Even with the difference in techniques between those used by Dobson et al. (1997) and those used in this paper and the lower temporal resolution of the Dobson et al. (1997) data set, a marked increase in terrigenous accumulation rate for this same time interval at Ceara Rise is apparent and compares reasonably with the patterns we observe at Site 999 (Fig. 5). For the Ceara Rise, the increase is thought to be associated with Andean uplift and increased Amazon River flow (Dobson et al., 1997). Sites 998 and 999, located in the western Caribbean, are likely too far away to be reflecting an Amazon source. However, Site 999 is in close proximity to the Magdalena Fan, which drains the northern Andes (Sigurdsson, Leckie, Acton, et al., 1997). It is difficult to resolve whether the increase in terrigenous accumulation at Site 999 (beginning at 38 Ma) precedes the increase at Ceara Rise, since the Ceara Rise data set is poorly resolved from 30 to 42 Ma (Fig. 5). Regardless, both the Atlantic and the Caribbean are apparently showing the same broad depositional pattern from both the Amazon and Magdalena drainage basins. Thus, these two locations serve as good circum-Andean tracers of tectonism.

Dispersed Ash

Dispersed ash accumulation rates (Figs. 3, 6) show three distinct periods of increased accumulation. Two of these periods are in the Paleocene (at 62–60 and 58–54 Ma) and are recorded at both Sites 999 and 1001. The younger (58–54 Ma) is through the Paleocene/Eocene boundary and may be causally related to the late Paleocene/ Eocene thermal maximum climatic event (Bralower et al., 1997).

These periods of increased deposition of dispersed ash occurred somewhat earlier at Site 999 than at Site 1001; however, Site 1001 has higher absolute accumulation rates (Fig. 3). The difference in timing probably is not caused by variations in age models; at both sites, the ages during these periods are tightly constrained (Sigurdsson, Leckie, Acton, et al., 1997). Also, the sedimentation rates at both sites were approximately the same during these times, especially between 62 and 60 Ma.

The major source of dispersed ash accumulation during both Paleocene maxima appears to be the Late Cretaceous Greater Antilles/ Cayman Volcanic Arc (Montgomery, 1998; Pindell and Barrett, 1990; Stykes et al., 1982; Wadge and Burke, 1983; White and Burke, 1980; see also discussion in Sigurdsson, Leckie, Acton, et al., 1997). This arc evolved as a result of a reversal in subduction polarity between 120 and 110 Ma (Draper et al., 1996; Draper and Gutierrez-Alonso, 1997), but volcanism did not cease until the early Eocene in

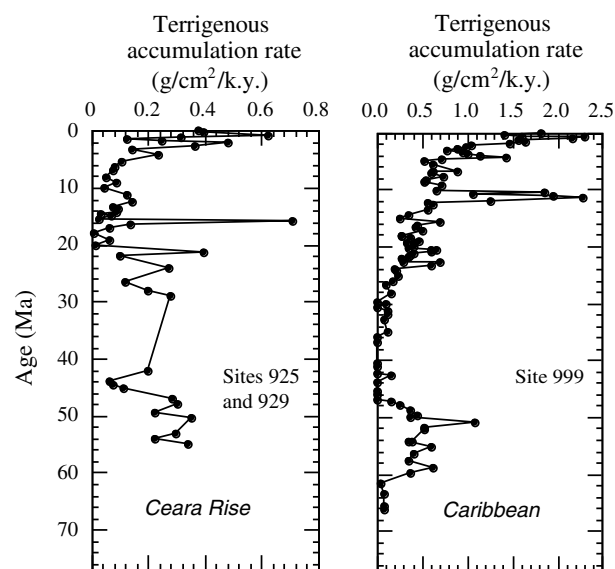


Figure 5. Terrigenous matter accumulation at Sites 925 and 929 on the Ceara Rise (Dobson et al., 1997) and Site 999 in the Caribbean.

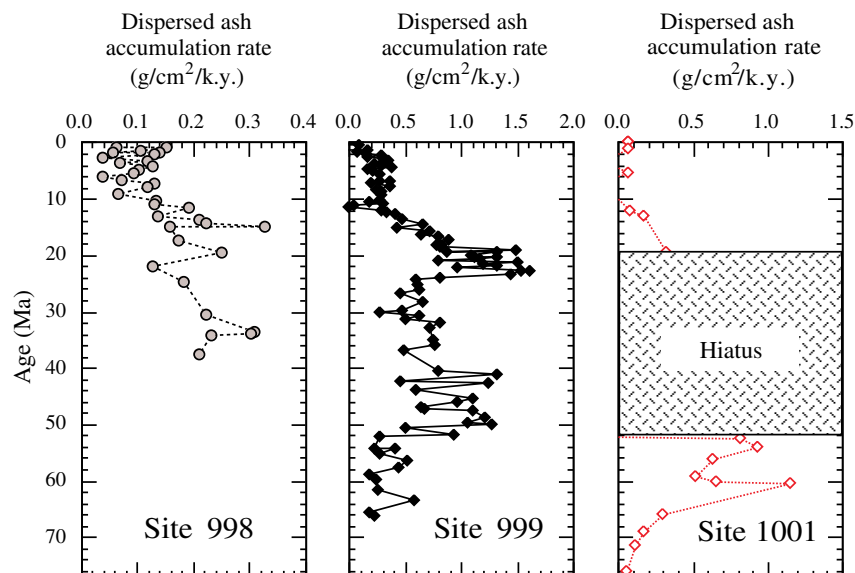


Figure 6. Dispersed ash accumulation rate at Sites 998 (shaded circles), 999 (solid diamonds), and Site 1001 (open diamonds) vs. age, plotted with expanded scales on the x-axes.

some of the Greater Antilles islands (Pindell and Barrett, 1990; Lewis and Draper, 1990). The Central American arc is not likely to be a major source of these Paleocene maxima because Site 999, located closest to Central America during this time (Pindell and Barrett, 1990), records lower dispersed ash accumulation (Fig. 3). Both Sites 998 and 1001 were closer than Site 999 to the Late Cretaceous Greater Antilles Arc (Pindell and Barrett, 1990), Site 1001 shows greater dispersed ash accumulation rates during these episodes than Site 999, and Site 998 also records a maximum in discrete ash layers at ~52 Ma.

The second volcanic episode was in the Eocene, between 50 and 40 Ma. The record of this event is only seen at Site 999 because of the hiatus at Site 1001 and the fact that samples older than 39 Ma were not analyzed for dispersed ash from Site 998. The source of the dispersed ash deposited between 50 and 40 Ma is most likely the Central American arc (Sigurdsson, Leckie, Acton, et al., 1997), which probably formed a continuous string of volcanic islands between South America and the Chortis block of Nicaragua during the Paleocene to middle Eocene (Maury et al., 1995).

The third episode of volcanism occurred in the Miocene between 22 and 14 Ma. The greatest accumulation by far is at Site 999, but the episode is also recorded at Site 998. The source is thought to be the Central American arc, similar to the source of the Eocene event (Sigurdsson, Leckie, Acton, et al., 1997). The volcanic activity was concentrated in the middle of Central America within the Chorotega block and gave rise to intensive volcanism (Escalante, 1990).

These dispersed ash records of volcanic activity agree well with the tectonic history of the region. Eruptive and intrusive calc-alkaline units are found in the Greater Antilles, such as the Mal Paso Formation and Palma Escrita Formation of Puerto Rico (Jolly et al., 1998), and in northern South America and Central America as seen in the volcanic agglomerate from the Tuira-Chucunaque Basin (Escalante, 1990; Frost et al., 1998). Crustal movement, which started in the early Tertiary and reached a climax in the early Eocene, caused uplift in northern Central America and throughout the northern Caribbean margin (Lewis and Draper, 1990). Arc volcanism in the eastern Greater Antilles commenced in the Cretaceous and terminated throughout the Eocene (depending on location), progressing from initial collision in Cuba to younger events of lesser effect to the west (Montgomery, 1998; Lewis and Draper, 1990; Pindell and Barrett, 1990).

Orogeny in Central America and western Columbia likely reached its peak during the late Miocene (Escalante, 1990). This activity gave rise to intense volcanism that is associated with the volcanic Aguacate, Rio Pey, and Paso Real Formations in Costa Rica, and other volcanic rocks in western Panama (Escalante, 1990). The broad timing of tectonic activity corresponds with the large Miocene accumulation of both dispersed ash and discrete ash observed at Sites 999 and 998. As described in Carey and Sigurdsson (Chap. 5, this volume), the extremely large volcanic eruptions responsible for the ash in the Caribbean Sea resulted in ejected material reaching stratospheric elevations, where wind flows from west to east (i.e., in the opposite direction of the lower level trade winds).

The Relationship between Dispersed Ash and Discrete Ash Layers

The record of discrete ash layers (Carey and Sigurdsson, 1998; Carey and Sigurdsson, Chap. 5, this volume) shows that the major volcanic episodes occurred in the Paleocene (65–60 Ma), Eocene (47–37 Ma), and Miocene (~17 Ma). Grain-size and shape analyses, along with modeling of ash transport mechanisms, indicate that these discrete ash layers most likely represent eruptions that exceeded 40 km in height and are associated with large volume ignimbrites (Carey and Sigurdsson, Chap. 5, this volume). The timing of these peaks in comparison with those for the dispersed ash accumulation rates indi-

cate that the discrete layers consistently lag temporally behind the dispersed ash accumulation. This is especially apparent at Site 999 (Fig. 7). At this site, dispersed ash maxima are seen between 52 and 48 Ma and again between 42 and 41 Ma, whereas discrete ash layers peak between 42 and 40 Ma and between 36 and 34 Ma. The lead-lag relationship is also seen between 22 and 10 Ma with the dispersed ash leading by ~2–4 Ma. At Site 998, the relationship is less pronounced, but can be observed in a dispersed ash accumulation rate peak at ~14 Ma followed by a 12 Ma peak in the ash layer accumulation (Fig. 7).

Various causes can be proposed for these relationships. One explanation is that perhaps there is not a true temporal relationship being observed, but rather that the discrete ash layers reflect volcanism at close proximity and the dispersed ash accumulation rates reflect volcanism at further distances in the circum-Caribbean region. For example, the maximum in ash layer accumulation at Site 998 at ~50 Ma corresponds with identically timed peaks in dispersed ash observed at Site 999 (Fig. 7). Similarly, the maxima in dispersed ash accumulation rates at Site 998 at 18 and 34 Ma correspond with ash layer accumulations at Site 999. However, even though the accumulation of the ash layers (in centimeters per million years) is comparable (~250 cm/m.y.) at Site 998 at 50 Ma and at Site 999 at 34 and 18 Ma, the corresponding dispersed ash maxima are greater at Site 999.

If the discrete ash at one site and dispersed ash at another are contemporaneous and receiving ash from the same source, this provides information regarding the transport mechanism and the distribution of volcanic sediments. To form discrete ash layers at these sites would require high intensity eruptions with column heights in excess of 40 km (Carey and Sigurdsson, Chap. 5, this volume). Particles in the umbrella region of such an eruption would be transported by the prevailing high-altitude wind direction (Carey and Sigurdsson, Chap. 5, this volume; Sigurdsson et al., 1980). Thus, the discrete ash was most likely transported in the stratosphere and the transport is stronger in the northward direction.

Another potential explanation is that the region experienced long periods of eruptions of small magnitude followed by intense large-

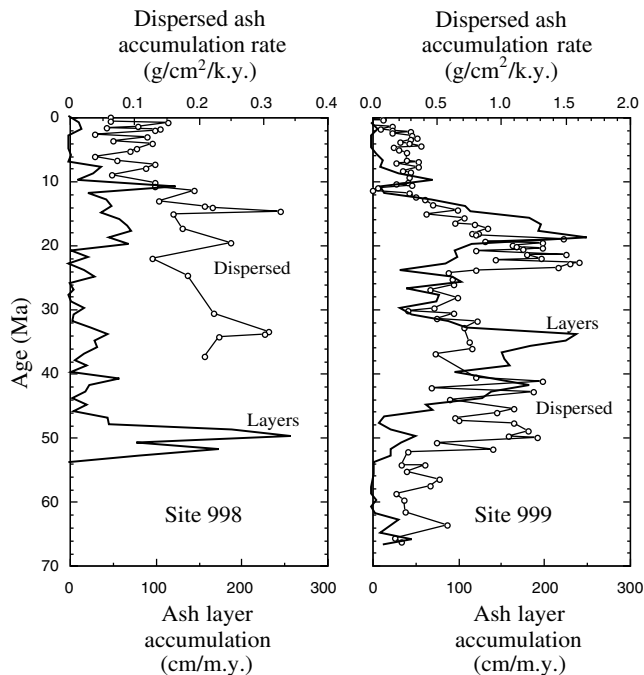


Figure 7. Accumulation rate of dispersed ash (open circles) and accumulation of ash layers (solid line) vs. age at Sites 998 and 999. Note that the dispersed ash temporally leads ash layers. Please see Carey and Sigurdsson (Chap. 5, this volume) for discussion of these layers.

scale explosive volcanic activity. According to Sigurdsson et al. (1980), small magnitude eruptions such as the 1979 eruption of Soufriere in St. Vincent do not form megascopic ash layers; they only contribute to the dispersed ash content of the sediment. Experience in the Lesser Antilles indicates that visible layers are formed from eruptions that produce total volumes much greater than 1 km³ (Sigurdsson et al., 1980).

In this context, the dispersed ash may represent erosion of smaller terrestrially deposited ash sediments, which was then followed by associated massive volcanism (Noble et al., 1974) that resulted in discrete ash layers. If this is the source of dispersed ash, we should expect that even though the percent terrigenous component is small, there would be some coincidence between the terrigenous and the dispersed ash accumulation rate peaks because production and transport of both the dispersed ash and terrigenous components are caused by the same physical mechanism (i.e., erosion). This is in fact observed at all three sites. At Sites 999 and 1001, the terrigenous accumulation rate peak at 58–60 Ma corresponds with peaks in the dispersed ash. At Site 999, from 50 to 52 Ma a peak in terrigenous accumulation rate coincides with a peak in dispersed ash accumulation rate. The erosional event referred to earlier at Site 998 at 34 Ma shows a dispersed ash accumulation rate increase occurring at the same time as the increase in the terrigenous accumulation rate. Thus, in addition to recording obvious volcanism, the dispersed ash maxima may also be indicators of erosional events and could be proxies for uplift in the area.

SUMMARY AND CONCLUSIONS

1. Site 998 experienced an erosional event, inferred from an increase in terrigenous accumulation rates, in the mid-Oligocene at ~35 Ma. This erosional event may reflect uplift in Guatemala (Weyl, 1980) that began during Oligocene time and increased through the middle Miocene orogeny (Morris et al., 1990).
2. Terrigenous sedimentation throughout the Caribbean Sea region has increased markedly in the last 10 m.y., with Site 999 beginning a steady increase since 28 Ma. This is probably caused by the rapid Neogene uplift in Hispaniola, Guatemala, and northwestern South America. The uplift in northwestern South America seems to be dominant, as reflected in a similar increase in terrigenous accumulation rates at Sites 925 and 929 on the Ceara Rise, which receives input from the Amazon River draining the Andes (Dobson et al., 1997) and Site 999, which receives input from the Magdalena River draining the northern Andes (Sigurdsson, Leckie, Acton, et al., 1997). The uplift is continuing to the present (Morris et al., 1990; Mann et al., 1990; Mann and Burke, 1984).
3. Volcanism resulted in an extremely large source of sediment to the Caribbean Sea, as evidenced by both the high amount of dispersed ash and the accumulation of discrete ash layers. Three periods of volcanism (Paleocene, Eocene, and Miocene) are recorded in both the dispersed ash and discrete ash layer records. Site 1001 shows the greatest absolute accumulation during the Paleocene. The greatest ash accumulation rate occurs at Site 999 during the Miocene and Eocene. The source of these episodes of volcanism is believed to be the Central American arc (Sigurdsson, Leckie, Acton, et al., 1997).
4. The maxima in discrete ash layer accumulation temporally lags the dispersed ash accumulation rate. The lag may be a reflection of distance from the source of volcanism with sites nearer to the volcanism having deposits of discrete ash layers and distal sites showing dispersed ash, or it may be indicative of uplift and erosion of smaller volume deposits (leading to the dispersed record) followed by long periods of intense volcanic activity (leading to the discrete record).

ACKNOWLEDGMENTS

We thank Haraldur Sigurdsson and Steven Carey for their input and support of this project, both during and after the cruise. We also thank our cheery fellow chemlab mates, Tim Lyons and Graham Pearson, for their insights during the cruise. Thanks also to the shipboard ODP technicians for their efforts during Leg 165, and in particular Dennis Graham, John Lee, and Don Sims for assistance in the chemistry and X-ray laboratories. Adila Jamil provided assistance in the Analytical Geochemistry Laboratory at Boston University. RWM thanks JOI/USSSP for their financial support; JLP acknowledges fellowship support from BU (Martin Luther King scholarship). Acquisition and maintenance of the JY170C ICP-ES supported by NSF EAR-9724282. Jerry Dickens, Gren Draper, and an anonymous reviewer provided comments on the manuscript that greatly helped us clarify our thoughts.

REFERENCES

- Bralower, T.J., Thomas, D.J., Zachos, J.C., Hirschmann, M.M., Röhl, U., Sigurdsson, H., Thomas, E., and Whitney, D.L., 1997. High-resolution records of the late Paleocene thermal maximum and circum-Caribbean volcanism: is there a causal link? *Geology*, 25:963–966.
- Burke, K., 1988. Tectonic evolution of the Caribbean. *Annu. Rev. Earth Planet. Sci.*, 16:201–230.
- Burke, K., Fox, P.J., and Sengor, A.M.C., 1978. Buoyant ocean floor and the evolution of the Caribbean. *J. Geophys. Res.*, 83:3949–3954.
- Carey, S.N., and Sigurdsson, H., 1998. Modeling of volcanic ash dispersal in the Western Caribbean: implications for the nature and location of explosive volcanism. *Eos*, 79 (Suppl.):172.
- Dobson, D.M., Dickens, G.R., and Rea, D.K., 1997. Terrigenous sedimentation at Ceara Rise. In Shackleton, N.J., Curry, W.B., Richter, C., and Bralower, T.J. (Eds.), *Proc. ODP, Sci. Results*, 154: College Station, TX (Ocean Drilling Program), 465–473.
- Donnelly, T.W., 1989. Geologic history of the Caribbean and Central America. In Bally, A.W., and Palmer, A.R. (Eds.), *The Geology of North America - An Overview*. Geol. Soc. Am., Geol. of North Am. Ser., A:299–321.
- Draper, G., Gutierrez, G., and Lewis, J.F., 1996. Thrust emplacement of the Hispaniola peridotite belt: orogenic expression of the mid-Cretaceous Caribbean arc polarity reversal? *Geology*, 24:1143–1146.
- Draper, G., and Gutierrez-Alonso, G., 1997. La estructura del Cinturon de Maimon en la isla de Hispaniola y sus implicaciones geodinamicas. *Rev. Soc. Geol. Esp.*, 10:79–97.
- Droxler, A.W., and Burke, K., 1995. Cenozoic gateway opening and closing in the Caribbean: control on interoceanic and interhemispheric exchange of water masses between the Atlantic and Pacific Oceans. *Eos*, 76 (Suppl.):53.
- Droxler, A.W., Cunningham, A.D., Roth, J.M., and Kameo, K., 1998. Linkage between carbonate bank foundering (Northern Nicaragua Rise), Late Middle Miocene establishment of the Caribbean current, and the initiation of NADW production. *Eos*, 79 (Suppl.):172.
- Duncan, W.M., and Hargraves, R.B., 1984. Plate tectonic evolution of the Caribbean region in the mantle reference frame. In Bonini, W.E., Hargraves, R.B., and Shagam, R. (Eds.), *The Caribbean-South American Plate Boundary and Regional Tectonics*. Mem.—Geol. Soc. Am., 162:81–84.
- Escalante, G., 1990. The geology of southern Central America and western Colombia. In Dengo, G., and Case, J.E. (Eds.), *The Caribbean Region*. Geol. Soc. Am., Geol. of North Am. Ser., H:201–230.
- Farrell, J.W., Raffi, I., Janecek, T.C., Murray, D.W., Levitan, M., Dadey, K.A., Emeis, K.-C., Lyle, M., Flores, J.-A., and Hovan, S., 1995. Late Neogene sedimentation patterns in the eastern equatorial Pacific. In Pisias, N.G., Mayer, L.A., Janecek, T.R., Palmer-Julson, A., and van Andel, T.H. (Eds.), *Proc. ODP, Sci. Results*, 138: College Station, TX (Ocean Drilling Program), 717–756.
- Frost, C.D., Schellekens, J.H., and Smith, A.L., 1998. Nd, Sr, and Pb isotopic characterization of Cretaceous and Paleogene volcanic and plutonic island arc rocks from Puerto Rico. In Likiak, E.G., and Larue, D.K. (Eds.), *Tectonics and Geochemistry of the Northeastern Caribbean*. Spec. Pap.—Geol. Soc. Am., 322:123–132.

- Gromet, L.P., Dymek, R.F., Haskin, L.A., and Korotev, R.L., 1984. The "North American Shale Composite:" its compilation, major and trace element characteristics. *Geochim. Cosmochim. Acta*, 48:2469–2482.
- Jolly, W.T., Lidiak, E.G., Schellekens, J.H., and Santos, H., 1998. Volcanism, tectonics, and stratigraphic correlations in Puerto Rico. In Likiak, E.G., and Larue, D.K. (Eds.), *Tectonics and Geochemistry of the Northeastern Caribbean*. Spec. Pap.—Geol. Soc. Am., 322:1–34.
- Lewis, J.F., and Draper, G., 1990. Geology and tectonic evolution of the northern Caribbean margin. In Dengo, G., and Case, J.E. (Eds.), *The Caribbean Region*. Geol. Soc. Am., Geol. of North Am. Ser., H:77–140.
- Lyle, M., Dadey, K.A., and Farrell, J.W., 1995. The late Miocene (11–8 Ma) eastern Pacific carbonate crash: evidence for reorganization of deep-water circulation by the closure of the Panama Gateway. In Pisias, N.G., Mayer, L.A., Janecek, T.R., Palmer-Julson, A., and van Andel, T.H. (Eds.), *Proc. ODP, Sci. Results*, 138: College Station, TX (Ocean Drilling Program), 821–838.
- Mann, P., and Burke, K.C., 1984. Neotectonics of the Caribbean. *Rev. Geophys. Space Phys.*, 22:309–362.
- Mann, P., Schubert, C., and Burke, K., 1990. Review of Caribbean neotectonics. In Dengo, G., and Case, J.E. (Eds.), *The Caribbean Region*. Geol. Soc. Am., Geol. of North Am. Ser., H:307–338.
- Maury, R.C., Defant, M.J., Bellon, H., de Boer, J.Z., Stewart, R.H., and Cotten, J., 1995. Early Tertiary arc volcanics from Eastern Panama. In Mann, P. (Ed.), *Geologic and Tectonic Development of the Caribbean Plate Boundary in Southern Central America*. Spec. Pap.—Geol. Soc. Am., 295:29–34.
- Montgomery, H., 1998. Paleogene stratigraphy and sedimentology of the North Coast, Puerto Rico. In Likiak, E.G., and Larue, D.K. (Eds.), *Tectonics and Geochemistry of the Northeastern Caribbean*. Spec. Pap.—Geol. Soc. Am., 322:177–192.
- Morris, E.L., Tanner, I., Meyerhoff, H.A., and Meyerhoff, A.A., 1990. Tectonic evolution of the Caribbean region: alternative hypothesis. In Dengo, G., and Case, J.E. (Eds.), *The Caribbean Region*. Geol. Soc. Am., Geol. of North Am. Ser., H:433–457.
- Murray, R.W., and Leinen, M., 1993. Chemical transport to the seafloor of the equatorial Pacific Ocean across a latitudinal transect at 135°W: tracking sedimentary major, trace, and rare earth element fluxes at the Equator and the Intertropical Convergence Zone. *Geochim. Cosmochim. Acta.*, 57:4141–4163.
- , 1996. Scavenged excess aluminum and its relationship to bulk titanium in biogenic sediment from the central Pacific Ocean. *Geochim. Cosmochim. Acta*, 60:3869–3878.
- Murray, R.W., Leinen, M., Murray, D.W., and Mix, A.C., 1995. Terrigenous Fe input and biogenic sedimentation in the glacial and interglacial equatorial Pacific Ocean. *Global Biogeochem. Cycles*, 9:667–684.
- Noble, D.C., McKee, E.H., Farrar, E., and Petersen, U., 1974. Episodic Cenozoic volcanism and tectonism in the Andes of Peru. *Earth Planet. Sci. Lett.*, 21:213–220.
- Peterson, L.C., Haug, G.H., King, J.W., and Murray, R.W., 1998. Rapid climate change in the Caribbean as recorded in Late Quaternary sediments of the anoxic Cariaco Basin. *Eos*, 79 (Suppl.):173.
- Pindell, J.L., and Barrett, S.F., 1990. Geologic evolution of the Caribbean region: a plate-tectonic perspective. In Dengo, G., and Case, J.E. (Eds.), *The Caribbean Region*. Geol. Soc. Am., Geol. North. Am. Ser., H:405–432.
- Schroeder, J.O., Murray, R.W., Leinen, J., Pflaum, R.C., and Janecek, T.R., 1997. Barium in equatorial Pacific carbonate sediment: terrigenous, oxide, and biogenic associations. *Paleoceanography*, 12:125–146.
- Sigurdsson, H., Leckie, R.M., Acton, G.D., et al., 1997. *Proc. ODP, Init. Repts.*, 165: College Station, TX (Ocean Drilling Program).
- Sigurdsson, H., Sparks, R.S.J., Carey, S.N., and Huang, T.C., 1980. Volcanogenic sedimentation in the Lesser Antilles arc. *J. Geol.*, 88:523–540.
- Stykes, L.R., McCann, W.R., and Kafka, A.L., 1982. Motion of Caribbean Plate during last 7 million years and implications for earlier movements. *J. Geol. Res.*, 87:10656–10676.
- Taylor, S.R., and McLennan, S.M., 1985. *The Continental Crust: Its Composition and Evolution*: Oxford (Blackwell Scientific).
- Wadge, G., and Burke, K., 1983. Neogene Caribbean Plate rotation and associated Central American tectonic evolution. *Tectonics*, 2:633–643.
- Weyl, R., 1980. *The Geology of Central America*: Berlin (Gebrüder Borntraeger).
- White, G.W., and Burke, K.C., 1980. Outline of the tectonic evolution of the Gulf of Mexico and Caribbean Region. *Houston Geol. Soc. Bull.*, 22:8–13.

Date of initial receipt: 22 June 1998

Date of acceptance: 8 February 1999

Ms 165SR-003